Journal of Materials Chemistry B

PAPER

View Article Online
View Journal | View Issue

Published on 24 February 2014. Downloaded by Anadolu University on 26/04/2014 05:27:29.

Cite this: J. Mater. Chem. B, 2014, 2, 3022

Improved immobilization of DNA to graphite surfaces, using amino acid modified clays†

Ali A. Ensafi,* Esmaeil Heydari-Bafrooei, Mohammad Dinari and S. Mallakpour

Assessment of the interaction of small molecules with DNA, hybridization assays for DNA sequence analysis and diagnostics and the investigation of DNA damage involves the immobilization of an array of oligonucleotides onto a solid substrate. Herein, a new nano sized DNA-based biosensor containing valine (Val) amino acid organo-modified Cloisite Na^+ as a new bionanohybrid film for the immobilization of DNA was developed. The Cloisite–Val organoclay was synthesized by a cation-exchange method, which involves the displacement of the sodium cations of Cloisite Na^+ with the ammonium ions of the Val-amino acid. The synthesized materials were characterized with different methods such as FT-IR spectroscopy, TEM, SEM, XRD and electrochemical impedance spectroscopy (EIS). The nanostructured film was deposited at the surface of a working graphite electrode and utilized for the surface modification with double-stranded DNA. It was found that the electrode modification with DNA and Cloisite–Val leads to an enhanced sensitivity in the DNA voltammetric detection compared with other modified electrodes that were used for this work. The efficiency of DNA immobilization was followed by means of EIS and voltammetry. Immobilization is much more rapid when using the Cloisite–Val modified graphite support than when employing conventional supports. The stability of the immobilized DNA over several days has been found to be much higher when using the new support than in preparations using conventional ones.

Received 22nd December 2013
Accepted 24th February 2014

DOI: 10.1039/c3tb21827a

www.rsc.org/MaterialsB

1. Introduction

In the last two decades, intense research effort has been paid to DNA biosensors. DNA diagnostics have become an important area of molecular biology and biotechnology studies.[1–3] The detection of specific base sequences in human, viral and bacterial nucleic acids is becoming increasingly important in several areas, with applications ranging from the detection of disease causing and food-contaminating organisms to forensic and environmental research and the monitoring DNA–small molecule interactions.[4–7]

Like other biosensors, DNA sensors are usually in the form of electrodes, chips, and crystals. Hence, interaction or hybridization on a sensory surface is a solid-phase reaction. Various techniques, including electrochemical methods, are currently employed for direct confirmation of hybridization or interaction.[8,9] Detection systems are being upgraded to produce more sensitive methods at faster rates.[10] Carbon surfaces are very good materials for electrochemical studies, such as biosensor applications, due to their special allotropes (graphite, diamond and fullerenes/nanotubes).[11] The often-cited advantages of carbon electrodes include low cost, wide potential window, relatively inert electrochemistry, and electrocatalytic activity for a variety of redox reactions.[12,13]

In order to prepare devices based on DNA, the first critical issue to face is related to the immobilization procedures on the surface of the transducer.[14] In view of the impressive advance in the applicability of DNA biosensors, it is important to further enhance the sensitivity of the system. This can be achieved by increasing the amount of immobilized DNA per unit array area. The development of DNA immobilization methodologies that strongly stabilize DNA on the electrode surface is one key factor in DNA biosensor design.[15] The sensor material and the degree of surface coverage, which directly influences the sensor response, are also critical issues in the development of a DNA electrochemical biosensor for rapid detection of DNA interaction and damage by hazardous compounds.

DNA can be immobilized on sensor surfaces with methods similar to those used for enzyme-based biosensors: adsorption,[16,17] covalent immobilization,[18–20] and avidin (or streptavidin)–biotin interactions.[21,22] These immobilization techniques also can be used to develop DNA microarrays.[23] Immobilization based on adsorption has been reported based on ionic interactions occurring between the negatively charged groups present on the DNA probe and positive charges covering the surface. Non-covalent forces affix the nucleic acid to such materials as nitrocellulose, nylon membranes, polystyrene or

Department of Chemistry, Isfahan University of Technology, Isfahan 84156-83111, Iran. E-mail: Ensafi@cc.iut.ac.ir; Fax: +98-311-3912350; Tel: +98-311-3913269

† Electronic supplementary information (ESI) available. See DOI: 10.1039/c3tb21827a

This journal is © The Royal Society of Chemistry 2014

Published on 24 February 2014. Downloaded by Anadolu University on 26/04/2014 05:27:29.

metal oxide surfaces such as palladium or aluminum oxide.[24,25] The positive charge can be obtained by means of covering the surface with cationic polycations[26,27] or a molecular monolayer functionalized by terminal amine groups.[28] Immobilization based on covalent attachment includes chemisorptions and attachment of DNA on functionalized surfaces.

Immobilizing DNA by means of clay minerals has attracted the attention of electrochemists. Clay minerals have many desirable properties as electrode surface modifiers: small particle size, large surface area-to-mass ratio, ion-exchange capacity, good intercalation, high stability, flexible adsorption capability and excellent felting property. In green chemistry terms, their environmentally friendly analytical protocols and devices, negligible waste, and nontoxic materials make clay minerals of considerable interest to the analytical community.[29,30]

Herein, we report for the first time the use of a nanohybrid of clay and a natural amino acid as a substrate for both covalent and electrostatic immobilization of DNA oligonucleotides. We chose Cloisite Na^+ as a kind of montmorillonite (MMT) clay and the amino acid valine (Val) as a natural amino acid for the preparation of a Cloisite–Val organoclay. The current research focuses on DNA immobilization on the Cloisite–Val modified electrode and provides a suitable platform for DNA biosensor fabrication.

2. Experimental section

2.1. Materials

A sodium-containing natural MMT was obtained from Southern Clay Products Inc., Texas, USA with the trade name Cloisite Na^+ and cation exchange capacity (CEC) = 92.6 meq. per 100 g. s-Valine ($C_5H_{11}NO_2$, 117.15 g mol^{-1}, 99%) and hydrochloric acid (HCl) were purchased from Merck Chemical Co. Analyte solutions were prepared from reagent grade chemicals with deionized water. A deoxyribonucleic acid sodium salt of salmon testes (ds-DNA, catalog no. D1626) and poly(diallyldimethylammonium chloride) (PDDA, low molecular weight) were purchased from Sigma (St. Louis, USA) and used as received. All other chemicals were of reagent grade.

2.2. Apparatus

Electrochemical and impedimetric measurements were performed with an Autolab PGSTAT 12, potentiostat/galvanostat in a conventional three-electrode electrochemical cell using pencil graphite (PG, 0.7 mm diameter, Pentel Co., LTD, Japan) as the working electrode, platinum wire as an auxiliary electrode, and an Ag/AgCl reference electrode in 3.0 mol L^{-1} KCl aqueous media. A standard one-compartment three-electrode cell of 10 mL capacity and a renewable pencil graphite electrode (PGE) was used in all the experiments, as described in Gigante *et al.*[32] A Noki pencil was used as a holder for the pencil graphite lead. Electrical contact with the lead was obtained by soldering a metallic wire to the metallic part. The pencil was held vertically with 12 mm of the lead extruded outside (9 mm of which was immersed in the solution). The convective transport was provided by a magnetic stirrer. All the electroanalytical measurements were performed at room temperature.

Electrochemical impedance spectroscopy measurements were carried out in the presence of 5.0 mmol L^{-1} $K_3[Fe(CN)_6]$/$K_4[Fe(CN)_6]$ as a redox probe in 0.1 mol L^{-1} KCl at a polarization potential of 0.20 V in the frequency range of 0.005 to 10^5 Hz and with an amplitude of 10 mV.

A pH meter, Metrohm (Model 827), with a glass electrode (filled with sat. KCl) was used for pH measurements.

2.3. Preparation of the organoclay

An organoclay of Cloisite–Val was synthesized by a cation-exchange method, which involves the displacement of the sodium cations of Cloisite Na^+ with the ammonium ions of the Val-amino acid, according to our previous study.[31] Briefly, two grams of Cloisite Na^+ was dispersed separately in 150 mL of hot deionized water for 6 h at 80 °C. The required amount of s-Val was protonated with a stoichiometric amount of concentrated HCl in 50 mL of deionized water and heated at 80 °C for 3 h. These two solutions were mixed and the contents were vigorously stirred for 6 h at 60 °C. The mixture was filtered through a Whatmman® filter paper and then washed about five times with deionized water to remove superficially protonated-tyrosine sorbed on the surface.

2.4. Materials characterization

Fourier transform infrared (FT-IR) spectra were recorded on a Jasco-680 (Japan) spectrophotometer with 2 cm^{-1} resolution. The KBr pellet technique was applied for monitoring changes in the FT-IR spectra of the samples in the range of 4000–400 cm^{-1}.

The interlayer spacing of Cloisite Na^+ and the Cloisite–Val organoclay was measured by an X-ray diffractometer (XRD) (Bruker, D8 Advance, Germany) with Cu Kα radiation (λ = 0.1542 nm) at 45 kV and 100 mA. The diffraction patterns were collected between 2θ of 1.2° and 10° at a scanning rate of 0.05° per min. The basal spacings were determined from the position of the $d(001)$ reflection. The d-spacing of the organic bionanoclays was analyzed using Bragg's equation ($n\lambda = 2d \sin\theta$).

The morphology of Cloisite Na^+ and the Cloisite–Val organoclay was examined by scanning electron microscopy (SEM) (XL30, Philips). The powdered sample was dispersed in H_2O, and then the sediment was dried at room temperature before gold coating. Transmission electron microscopy (TEM) images were obtained using a Philips CM 120 microscope with an accelerating voltage of 100 kV.

2.5. Film assembly

The surface of the PGE was pretreated by applying +1.40 V for 60 s in a 0.5 mol L^{-1} acetate buffer (pH 4.8). A 5% (w/v) colloidal dispersion of Cloisite–Val was prepared by stirring the material in toluene. To assemble the Cloisite–Val/DNA layer-by-layer films, the PGE was alternately immersed into the Cloisite–Val solution for 30 min and into the DNA solution (1.0 mg mL^{-1}, in 0.02 mol L^{-1} tris buffers at pH 7.0 containing 0.02 mol L^{-1} NaCl and 1.0 mmol L^{-1} EDTA) for 10 min with intermediate water washing and nitrogen stream drying. The bare Cloisite–Val–

Published on 24 February 2014. Downloaded by Anadolu University on 26/04/2014 05:27:29.

modified PGEs were prepared by following the procedure above without any DNA incorporation into the clay matrix. The prepared Cloisite–Val/DNA films were overoxidized by performing DPV measurements between +0.50 V and +1.40 V at a 50 mV pulse amplitude and 10 mV step potential until a steady state response was obtained.

2.6. Transduction

A freshly prepared PGE surface was used for each electrochemical measurement. All the experiments were performed at room temperature. All the buffer solutions contained 20 mmol L^{-1} NaCl to establish a constant low ionic strength. The determination of ds-DNA oxidation on the surface of PG, Cloisite–Val/DNA and other modified electrodes was performed with a positive-going differential pulse potential scan (from 0.40 to 1.40), using a pulse amplitude of 50 mV, a modulation time of 0.05 s, and a step potential of 8 mV in the blank solution (0.5 mol L^{-1} acetate buffer (pH 4.8) containing 0.02 mol L^{-1} NaCl). The raw data were treated using the Savitzky and Golay filter (level 2) of the General Purpose Electrochemical Software (GPES) of Eco Chemie (The Netherlands), followed by the GPES software moving average baseline correction, using a "peak width" of 0.01. The procedure was repeated using a new PGE.

3. Results and discussion

3.1. Synthesis and characterization

α-Amino acids are one of the major building blocks of living systems, being the principal components of all naturally occurring peptides and proteins. The use of these compounds in hybrid materials increases the biocompatibility of such systems and allows interactions with biological organisms, which is advantageous for bioresorbable sutures, screws or plates, tissue engineering scaffolds and drug delivery systems.[32–34] If amino acids are used as a modifier for organo-modification of clays, they can be expected to be compatible with a protein/biopeptide matrix. When compared with a chemically synthesized modifier, amino acid biosurfactants have the important advantages of biodegradability, low toxicity and various possible structures.[32–34] In this study, a Cloisite–Val organoclay was prepared *via* a simple and environmentally friendly ion-exchange method in aqueous solution. Our interest in applying an amino acid as a swelling agent stems from the fact that the amine group of an amino acid can provide a cation ($-NH_3^+$) which can form an ionic bond with the negatively charged silicate layers of MMT as well as an electrostatic interaction and covalent bond with DNA chains for the construction of DNA-based biosensors.

3.2. FT-IR spectroscopy

In the FT-IR spectrum of Cloisite Na^+, the absorption bands at about 3100–3700 cm^{-1} are owing to the O–H stretching and the stretching band of hydrogen-bonded water. A weak broad peak at 1639 cm^{-1} is related to the H–O–H bending region. The characteristic peaks at 1115 cm^{-1} and 1042 cm^{-1} are due to the out-of-plane Si–O stretching and in-plane Si–O stretching for layered silicates, respectively. Other characteristic vibration peaks at 524 and 468 cm^{-1} are for the bending vibrations of Si–O and Al–O, respectively (Fig. 1). For the organoclay, absorption peaks were observed originating from the amino acid molecules. For example, the shoulder FT-IR peaks in the range of 2500–3700 cm^{-1} are related to OH stretching of the –COOH group (Fig. 1). The peak at 2960 cm^{-1} is attributed to the C–H stretching vibration of an aliphatic hydrocarbon and the peak at around 1700 cm^{-1} it is related to the carbonyl group of the amino acid.

3.3. X-ray diffraction

The most common technique used to analyze the clay materials is XRD, which measures the interlayer *d*-spacing. The XRD patterns of Cloisite Na^+ and Cloisite–Val are shown in Fig. 2. Pristine Cloisite Na^+ has an XRD peak at $2\theta = 7.56°$ which was caused by the diffraction of the (001) crystal surface of the layered silicates, equaling a *d*-spacing of 1.17 nm. In the XRD pattern of Cloisite–Val, the *d*-spacing of the organoclay was 1.49 nm based on Bragg's Law. An increase in the interlayer distance leads to a shift of the reflection toward lower angles and confirmed that intercalation and surface modification of Cloisite Na^+ had taken place. This means that the basic structure of Cloisite Na^+ is kept, the layers are only propped open, and the basal spacing increased appreciably, providing evidence that intercalation has occurred.

3.4. SEM and TEM study

SEM was used to investigate the morphology of Cloisite Na^+ and the organo-modified clay. The SEM image of Cloisite Na^+ before and after modification with Val is reported in our previous study.[31] According to the results of the obtained data, there are not many morphologic differences in the organoclay despite the obvious variation observed in the XRD measurements. Cloisite Na^+ shows a massive, aggregated morphology and in some instances, there are some bulky flakes. The morphology of the clay modified with Val had more smaller sized fragments formed with irregular shapes.

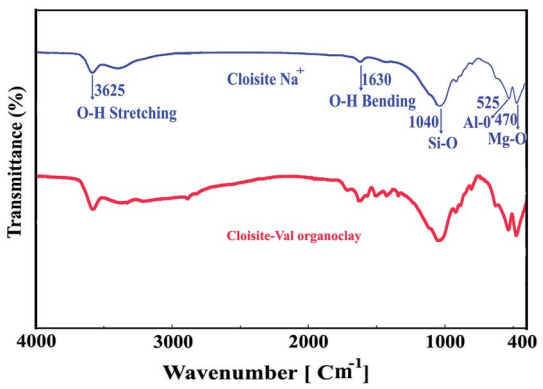

Fig. 1 FT-IR (KBr) spectra of Cloisite Na^+ and the organo-modified clay.

 This journal is © The Royal Society of Chemistry 2014

Published on 24 February 2014. Downloaded by Anadolu University on 26/04/2014 05:27:29.

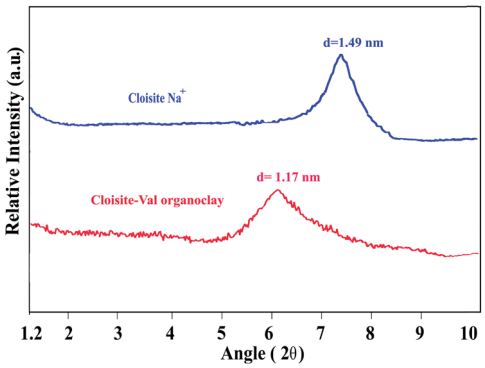

Fig. 2 XRD patterns of Cloisite Na^+ and Cloisite–Val.

TEM allows for direct examination of microstructural features resulting from the transformation of clays to organoclays. It has been reported that the layered-structure images of untreated Cloisite Na^+ cannot be observed with TEM.[35,36] It was supposed that for an unmodified clay, there is water adsorbed on exchangeable cations such as Na^+. The high vacuum of TEM and the high-energy beam can remove the water, which makes the layered structure collapse and forbids the structures from being readily observed. Contrasting with unmodified Cloisite Na^+, the clay modified with the Val-amino acid shows a layered structure, and the $d(001)$ basal spacing is around 12 to 15 Å (Fig. 3). This is almost in general agreement with the XRD results.

3.5. The oxidation of ds-DNA

To evaluate the effect of the Cloisite–Val film on the amount of DNA immobilized on the PG surface, a Cloisite–Val–PG electrode was constructed and oxidation voltammograms of guanine and adenine were obtained and compared with other modified electrodes that are often used for the immobilization of DNA (MWCNT–PDDA/PG and MWCNT–CHIT/PG). One of the best molecules which are used in the immobilization of DNA on carbon surfaces are carbon nanotubes (CNTs). CNTs are widely used in the fabrication of immunosensors because of their high electrical conductivity, high chemical stability, and extremely high mechanical strength. DNA is an important biological polymer, which is classified as a natural and negatively charged polyelectrolyte due to its phosphate groups. It can be immobilized onto carbon nanotubes *via* covalent and non-covalent interactions.[37] However, the results are not good enough because negatively charged CNTs repulse the negatively charged DNA.[38] To overcome this problem, a cationic polyelectrolyte such as, poly(diallyldimethylammonium chloride) (PDDA), chitosan (CHIT) and polyethylenimine is used as dispersant of the CNTs.[39] The positively charged PDDA, CHIT and polyethylenimine coats the negatively charged surface of the CNTs by an electrostatic interaction. The polyelectrolyte molecules can combine considerably well with DNA to form DNA films. The CNTs not only display unique electron transfer properties that induce the conductivity of PDDA and improve the electron transfer characteristics, they also increase the amount of PDDA deposited on the electrode.

In order to examine the electrochemistry of ds-DNA at various electrode conditions, several experiments were performed. The conditions for the immobilization and oxidation experiments of ds-DNA on the surface of PG, MWCNT–PDDA/PG and MWCNT–CHIT/PG electrodes are discussed elsewhere.[4,5] First of all, the experimental parameters affecting the sensitivity were optimized and the experimental results are shown in the ESI.† The guanine and adenine bases of ds-DNA were oxidized on the surface of carbon electrodes at anodic potentials in acidic media.[4] This oxidation process is used in the detection of small molecules that interact with ds-DNA. Under the conditions of the experiment, the redox behavior of the original ds-DNA-immobilized PGE exhibited two oxidation processes of guanine (*ca.* +1.02 V) and adenine (*ca.* +1.28 V) residues (Fig. 4a). When DNA/MWCNT–PDDA/PG and DNA/MWCNT–CHIT/PG electrodes were used as the working electrode, the oxidation of the guanine and adenine bases of ds-DNA were seen at peak potential values of +0.91 and +1.21 V (*vs.* Ag/AgCl) in 0.5 mol L^{-1} ABS containing 20.0 mmol L^{-1} NaCl respectively (Fig. 4b and c). A shift of approximately 100 mV was observed in the oxidation peak potentials of the guanine and adenine bases of ds-DNA compared with bare PG. For comparison, the DNA/Cloisite–Val modified PG electrode was also prepared and used in the oxidation experiments. The

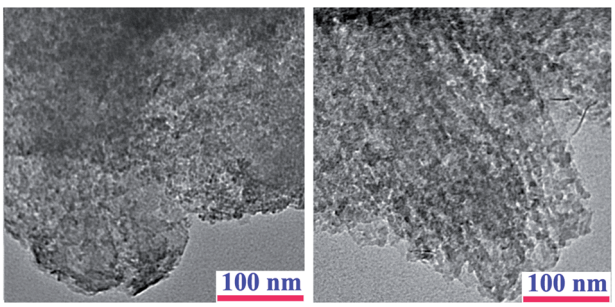

Fig. 3 TEM images of the modified clay with Val.

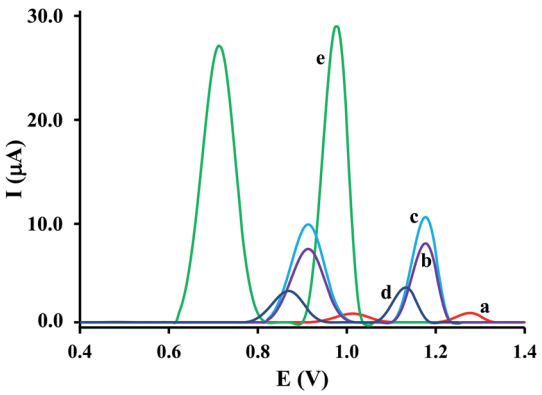

Fig. 4 Differential pulse voltammograms of guanine and adenine at the surface of (a) DNA–PGE, (b) DNA/MWCNT–CHIT/PGE, (c) DNA/MWCNT–PDDA/PGE (d) DNA/Cloisite/PGE, and (e) DNA/Cloisite–Val/PGE. Conditions: scanning potential between +0.40 and +1.40 V in an acetate buffer (pH 4.8).

Published on 24 February 2014. Downloaded by Anadolu University on 26/04/2014 05:27:29.

oxidation of ds-DNA was observed on the surface of the DNA/Cloisite–Val/PG electrode at peak potential values of +0.72 and +0.93 V (*vs.* Ag/AgCl) in a 0.5 mol L^{-1} acetate buffer containing 20.0 mmol L^{-1} NaCl respectively (Fig. 4e). It can be concluded that the Cloisite–Val nanocomposite-modified PG shows an electrocatalytic property and causes a potential shift in the oxidation peak potential of guanine and adenine to more cathodic values. This positive (catalytic) shift is approximately 300 mV. The electron transfer reaction between the Cloisite–Val electrodes and the guanine (or adenine) base of ds-DNA is faster than that of the reaction between the other modified electrodes that are often used for the immobilization of DNA (bare PG, MWCNT–PDDA/PG and MWCNT–CHIT/PG) and the guanine (or adenine) base of ds-DNA. On the other hand, the oxidation peak currents of the guanine and adenine bases of ds-DNA on the surface of Cloisite–Val were increased by about 32, 4 and 3 times according to the bare PG, MWCNT–CHIT/PG and MWCNT–PDDA/PG electrodes, respectively. An increase in the guanine moiety response at DNA/Cloisite–Val compared to simple bare PG, MWCNT–PDDA/PG and MWCNT–CHIT/PG is of interest for DNA detection. It is expected that the obvious increase in the detecting signal of the guanine (or adenine) base of ds-DNA is due to the participation of certain surface functional groups of the amino acid which increase the amount of DNA immobilization.

3.6. Electrochemical characteristics of the DNA marker

$Co(phen)_3^{3+}$ was used as an electroactive indicator to detect the DNA molecule using cyclic voltammetry. Table 1 shows the current and potential data of the oxidation differential pulse signal of $Co(phen)_3^{3+}$ obtained at the DNA/Cloisite–Val/PGE, Cloisite–Val modified PG and the other modified electrodes which are often used for the immobilization of DNA. Concerning the PGEs covered with nanomodifiers, the peak potential data for the DNA marker show a positive (catalytic) shift at both the MWCNT and Cloisite–Val modified electrodes, but this shift is more pronounced for the electrode modified with Cloisite–Val. The DNA deposited at the Cloisite–Val layer leads to a further increase in the $Co(phen)_3^{3+}$ peak current compared with the other electrodes (Table 1). Hence, the nanostructured Cloisite–Val film used can be covered effectively by ds-DNA. The efficiency of the Cloisite–Val composite coverage could be due to the better access of the marker particles to the DNA within the nanostructured films with an enhanced active surface area. The higher efficiency of DNA/Cloisite–Val/PGE compared to other modified PGEs is evidently due to the participation of certain functional groups of the amino acid at the adsorption of DNA. Thus, the amperometric response obtained with the DNA/Cloisite–Val/PG electrode proves that modification of the electrode with Cloisite–Val results in an increase in the DNA immobilization capacity and sensitivity. This offers an attractive prospect for using such films in DNA damage assays and DNA–molecule interactions.

The dependence of the peak current of $Co(phen)_3^{3+}$ on the accumulation time follows a typical adsorption isotherm shape with signal saturation from about 90 s for the DNA/Cloisite–Val modified PGE and about 300 s for the MWCNT modifiers. On the other hand, the kinetics of the accumulation of the DNA marker on Cloisite–Val has a faster isotherm in contrast to MWCNT-modified PGEs. In accordance with the data in Table 1, the modification of the bare PGE electrodes with a simple nanostructured film of MWCNT and Cloisite–Val leads to an increase in the $Co(phen)_3^{3+}$ signal due to its adsorption (on MWCNT and Cloisite–Val) or electrostatic chemisorption (on Cloisite–Val).

Table 1 Peak current and peak potential of the marker $Co(phen)_3^{3+}$ obtained after its 120 s accumulation from a 0.10 μmol L^{-1} solution in PBS (pH 7.0) before and after the modification of the corresponding PGE

Electrode	I_p (μA)	E_p (V)
Bare PGE	0.21 ± 0.05	−0.120
DNA/PGE	2.01 ± 0.21	−0.118
DNA/PDDA–MWCNT/PGE	4.23 ± 0.28	−0.129
DNA/CHIT–MWCNT/PGE	2.94 ± 0.17	−0.127
Cloisite–Val/PGE	2.04 ± 0.23	−0.132
DNA/Cloisite–Val/PGE	12.32 ± 0.52	−0.139

3.7. Electrochemical impedance spectroscopy

Previous studies have revealed that the amount of the assembly of nucleic acids on the support can be followed by electrochemical impedance spectroscopy, EIS.[26] Fig. 5 shows a Nyquist plot of impedance for PGE electrodes with different modifiers. In the Nyquist plot of the impedance spectra, the semicircular portion at higher frequencies corresponds to the electron-transfer-limited process and the linear portion seen at lower frequencies may be ascribed to the diffusion. The increase in the diameter of the semicircle reflects the increase in the interfacial charge-transfer resistance (*Rct*). In general, modification of the PG electrode with nanomodifiers causes a decrease in the surface impedance but on the other hand, DNA enhances the impedance. As shown in Fig. 5A, the effect of the DNA nanomodifier composite is different. The *Rct* of the bare PG electrode was 5200 Ω and the value decreased to 2800 and 3700

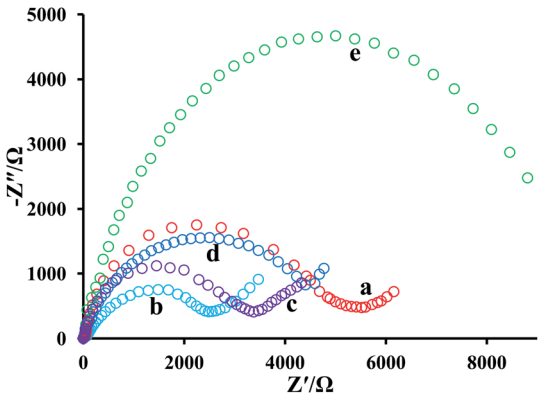

Fig. 5 Impedance spectra of (a) bare PGE, (b) MWCNT–PDDA/PGE, (c) Cloisite–Val/PGE, (d) DNA/MWCNT–PDDA/PGE, and (e) DNA/Cloisite–Val/PGE.

This journal is © The Royal Society of Chemistry 2014

Published on 24 February 2014. Downloaded by Anadolu University on 26/04/2014 05:27:29.

Ω with the deposition of PDDA–MWCNT and Cloisite–Val, respectively. After the immobilization of ds-DNA on PDDA–MWCNT and Cloisite–Val, the value of *Rct* increased to 5000 and 10 000 Ω, respectively. The increase in *Rct* is due to the immobilization of negatively charged ds-DNA on the electrode surface, resulting in a negatively charged interface that electrostatically repels the negatively charged redox probe $[Fe(CN)_6]^{3-/4-}$ and inhibits interfacial charge-transfer.[26] As shown in Fig. 5, the increase in *Rct* after the immobilization of DNA on the Cloisite–Val-modified PGE was greater compared with MWCNT. The EIS data shows that the nanostructured Cloisite–Val film has a superior ability for the immobilization of DNA on the surface. This feature is novel in the electrochemical detection of ds-DNA damage.

3.8. Effect of ionic strength

It is well known that interactions are effected by the ionic strength of the solution when the binding mode of the molecules with DNA is an electrostatic mode. At low ionic strength values, the electrostatic interaction mode between a molecule and the negative phosphate backbone of DNA is predominant, and conversely, at high ionic strength values, the negative charges of DNA phosphates are shielded and consequently, the electrostatic interaction is decreased. Thus, the effect of the ionic strength on the interaction of the nanostructured Cloisite–Val film with DNA was addressed by DPV in the NaCl concentration range from 0 to 100 mM. For this purpose, the Cloisite–Val/DNA layer-by-layer film was assembled using alternate immersion of the PGE into the Cloisite–Val solution for 30 min and into the DNA solution (1.0 mg mL^{-1}, in 0.02 mol L^{-1} tris buffers at pH 7.0 containing different concentration of NaCl and 1.0 mmol L^{-1} EDTA) for 10 min with intermediate water washing and nitrogen stream drying. In Fig. 6, experiments performed at both low (20.0 mM NaCl) and high (100.0 mM NaCl) ionic strengths are shown. As shown in Fig. 6, the current of guanine oxidation decreased by increasing the NaCl concentration. This fact suggests that DNA can interact electrostatically with the Cloisite–Val film and when the charges of the phosphate groups present in DNA are shielded, the interaction decreases and the amount of immobilized DNA diminishes.

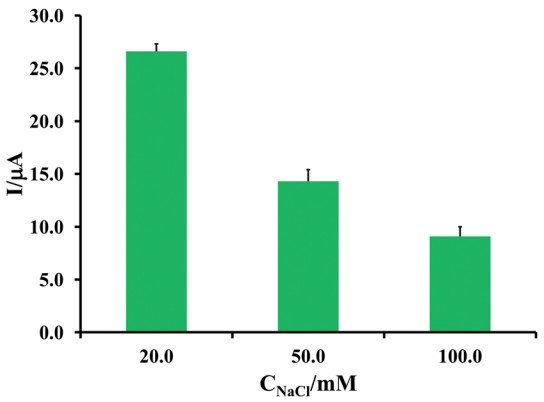

Fig. 6 Effect of NaCl concentration on the immobilization of 1.0 μg mL^{-1} DNA on the DNA/Cloisite–Val/PGE. Immobilization time: 10 min.

3.9. Stability of the biosensor

The DNA marker signal measurement was repeated over several days and the same biosensor was used to test the sensor stability. Between the measurements, the sensors were stored under dry conditions in open air and at room temperature. The working stability is characterized by an RSD value of the marker peak current obtained from 4 consecutive measurements, where the RSD values are 9% and 10% for the DNA/MWCNT–PDDA/PG and DNA/MWCNT–CHIT/PG electrodes, respectively. The total stability was tested during a 19 day period by measuring the marker signal every 3rd day. The RSD values reached 19% ($n = 10$) for the DNA/MWCNT–PDDA/PG and 27% ($n = 10$) for DNA/MWCNT–CHIT/PG electrode. In the case of the DNA/Cloisite–Val/PG modified electrode, the working and total stability is characterized by an RSD value of 4% ($n = 4$) and 5% ($n = 6$), respectively. This improved stability can satisfy a voltammetric assay of the interactions of the surface attached ds-DNA compared with other electrodes. It was not possible to use the electrodes for more than one measurement and they, therefore, had to be replaced each time.

4. Conclusions

In the work discussed in this report, a clay modified with the amino acid valine has been devised for the effective immobilization of DNA on graphite electrodes. The Cloisite–Val modified electrodes have shown to be an interesting support for DNA immobilization. The existence of amine groups in amino acid structures can dramatically improve immobilization rates by covalent immobilization. Moreover, the storage stability of the immobilized DNA was better than with conventional supports. Therefore, this support can be recommended as a new tool for DNA immobilization in DNA hybridization, damage and interaction assays.

Acknowledgements

The authors wish to thank the Research Council of Isfahan University of Technology (IUT), the Center of Excellence in Sensor and Green Chemistry, and the Iranian Nanotechnology Initiative Council for their support.

References

1 D. P. Little, T. J. Cornish, M. J. O'Donnell, A. Braun, R. J. Cotter and H. Köster, *Anal. Chem.*, 1997, **69**, 4540.
2 P. B. Monaghan, K. M. McCarney, A. Ricketts, R. E. Littleford, F. Docherty, W. E. Smith, D. Graham and J. M. Cooper, *Anal. Chem.*, 2007, **79**, 2844.
3 E. Donatin and M. Drancourt, *Med. Mal. Infect.*, 2012, **42**, 453.
4 A. A. Ensafi, M. Amini and B. Rezaei, *Sens. Actuators, B*, 2013, **177**, 862.

Published on 24 February 2014. Downloaded by Anadolu University on 26/04/2014 05:27:29.

5 A. A. Ensafi, E. Heydari-Bafrooei and B. Rezaei, *Biosens. Bioelectron.*, 2013, **41**, 627.
6 A. Dey, A. Kaushik, S. K. Arya and S. Bhansali, *J. Mater. Chem.*, 2012, **22**, 14763.
7 A. A. Ensafi, E. Heydari-bafrooei and M. Amini, *Biosens. Bioelectron.*, 2012, **31**, 376.
8 K. R. Meier and M. Gratzel, *ChemPhysChem*, 2002, **3**, 371.
9 F. Patolsky, A. Lichtenstein and I. Willner, *J. Am. Chem. Soc.*, 2001, **123**, 5194.
10 R. M. Kong, Z. L. Song, H. M. Meng, X. B. Zhang, G. L. Shen and R. Q. Yu, *Biosens. Bioelectron.*, 2014, **54**, 442.
11 R. L. McCreery, *Chem. Rev.*, 2008, **108**, 2646.
12 A. Walcarius, *TrAC, Trends Anal. Chem.*, 2012, **38**, 79.
13 Z. Peng, D. Zhang, L. Shi and T. Yan, *J. Mater. Chem.*, 2012, **22**, 6603.
14 M. I. Pividori, A. Merkoc and S. Alegret, *Biosens. Bioelectron.*, 2000, **15**, 291.
15 A. M. O. Brett, in *Bioelectrochemistry: Fundamentals, Experimental Techniques and Applications* ed. P. Bartlett, John Wiley & Sons, Ltd, 2008, ch. 12, p. 416.
16 C. M. A. Brett, A. M. O. Brett and S. H. P. Serrano, *J. Electroanal. Chem.*, 1994, **366**, 225.
17 M. L. Pedano and G. A. Rivas, *Electrochem. Commun.*, 2004, **6**, 10.
18 X. Jianga and X. Lin, *Analyst*, 2005, **130**, 391.
19 B. P. Corgier, A. Laurent, P. Perriat, L. J. Blum and C. A. Marquette, *Angew. Chem., Int. Ed.*, 2007, **46**, 4108.
20 A. Ruffien, M. Dequaire and P. Brossier, *Chem. Commun.*, 2003, 912.
21 R. M. Iost and F. N. Crespilho, *Biosens. Bioelectron.*, 2012, **31**, 1.
22 D. J. Chung, K. C. Kim and S. H. Choi, *Appl. Surf. Sci.*, 2011, **257**, 9390.
23 N. Zammatteo, L. Jeanmart, S. Hamels, S. Courtois, P. Louette, L. Hevesi and J. Remacle, *Anal. Biochem.*, 2000, **280**, 143.
24 J. R. Fernandes, D. H. Grant and M. Ozsoz, *Anal. Chem.*, 1997, **69**, 4056.
25 J. Wang, X. Cai, G. Rivas, H. Shiraishi and N. Dontha, *Biosens. Bioelectron.*, 1997, **12**, 587.
26 A. A. Ensafi, E. Heydari-Bafrooei and B. Rezaei, *Anal. Chem.*, 2013, **85**, 991.
27 A. A. Ensafi, M. Amini and B. Rezaei, *Biosens. Bioelectron.*, 2014, **53**, 43.
28 C. Douarche, R. Cortès, C. H. Villeneuve, S. J. Roser and A. Braslau, *J. Chem. Phys.*, 2008, **128**, 1.
29 C. Mousty, *Appl. Clay Sci.*, 2004, **27**, 159.
30 J. Zima, J. Barek and J. Labuda, *Electroanalysis*, 2006, **18**, 163.
31 S. Mallakpour and M. Dinari, *Appl. Clay Sci.*, 2011, **51**, 353.
32 A. Gigante, C. Chillemi, C. Bevilacqua, F. Greco, F. Bisaccia and A. M. Tamburro, *J. Mater. Sci.: Mater. Med.*, 2003, **14**, 717.
33 M. A. Pilkington-Miksa, M. J. Writer, S. Sarkar, Q. H. Meng, S. E. Barker, P. A. Shamlou, H. C. Hailes, S. L. Hart and A. B. Tabor, *Bioconjugate Chem.*, 2007, **18**, 1800.
34 G. Tosi, L. Costantino, F. Rivasi, B. Ruozi, E. Leo, A. V. Vergoni, R. Tacchi, A. Bertolini, M. A. Vandelli and F. Forni, *J. Controlled Release*, 2007, **122**, 1.
35 S. Mallakpour and M. Dinari, *J. Therm. Anal. Calorim.*, 2013, **111**, 611.
36 Y. Xi, R. L. Frost, H. He, T. Kloprogge and T. Bostrom, *Langmuir*, 2005, **21**, 8675.
37 P. G. He and M. Bayachou, *Langmuir*, 2005, **21**, 6086.
38 M. J. Gong, T. Han, C. X. Cai, T. H. Lu and J. Y. Du, *J. Electroanal. Chem.*, 2008, **623**, 8.
39 N. Li, H. W. Zhao, R. Yuan, K. F. Peng and Y. Q. Chai, *Electrochim. Acta*, 2008, **54**, 235.

This journal is © The Royal Society of Chemistry 2014